Katholieke Universiteit Leuven

Departement Elektrotechniek ESAT-SISTA/TR 12-45

Intercarrier Interference in DSL Networks due to Asynchronous DMT transmission [1]

Rodrigo B. Moraes, Paschalis Tsiaflakis and Marc Moonen[2]

February 2012
Submitted for publication for IEEE Transactions on Signal Processing.

[1]This report is available by anonymous ftp from *ftp.esat.kuleuven.ac.be* in the directory *pub/sista/rmoraes/reports/12-45.pdf*

[2]K.U.Leuven, Dept. of Electrical Engineering (ESAT), Research group SISTA, Kastelpark Arenberg 10, 3001 Leuven, Belgium, Tel. 32/16/32 17 09, Fax 32/16/32 19 70, WWW: *http://www.esat.kuleuven.ac.be/sista*. E-mail: *rodrigo.moraes@esat.kuleuven.be*. This research work was carried out at the ESAT Laboratory of the KU Leuven, in the frame of KU Leuven Research Council CoE EF/05/006 Optimization in Engineering (OPTEC) and PFV/10/002 (OPTEC), Concerted Research Action GOA-MaNet, the Belgian Programme on Interuniversity Attraction Poles initiated by the Belgian Federal Science Policy Office IUAP P6/04 (DYSCO, Dynamical systems, control and optimization, 2007-2011), Research Project FWO nr.G.0235.07(Design and evaluation of DSL systems with common mode signal exploitation) and IWT Project PHANTER: PHysical layer and Access Node TEchnology Revolutions: enabling the next generation broadband network. The scientific responsibility is assumed by its authors.

Intercarrier Interference in DSL Networks due to Asynchronous DMT transmission

Rodrigo B. Moraes*, Paschalis Tsiaflakis and Marc Moonen

Abstract

In this correspondence we focus on the effects of intercarrier interference (ICI) in digital subscriber lines (DSL) systems due to asynchronous discrete multitone (DMT) transmission and its impact on dynamic spectrum management (DSM). DSM aims to optimally allocate per-user transmit power so that the effect of multi-user interference, i.e. crosstalk, is minimized and the capabilities of the network are maximized. ICI arises when the the DMT blocks of interfering users in the network are not aligned in time and it significantly impacts the system performance. Our contribution is the derivation of aa accurate model for the effect of the ICI. We propose both an ICI model based on the particular delay between two users and an ICI model averaged over the delays between two users. Simulation results show that an accurate characterization of the ICI positively impacts the performance of DSM solutions.

Index Terms

SPC-TDLS, SPC-MULT, SPC-CRDS.

This research work was carried out at the ESAT Laboratory of the KU Leuven, in the frame of KU Leuven Research Council CoE EF/05/006 Optimization in Engineering (OPTEC) and PFV/10/002 (OPTEC), Concerted Research Action GOA-MaNet, the Belgian Programme on Interuniversity Attraction Poles initiated by the Belgian Federal Science Policy Office IUAP P6/04 (DYSCO, Dynamical systems, control and optimization, 2007-2011), Research Project FWO nr.G.0235.07(Design and evaluation of DSL networks with common mode signal exploitation) and IWT Project PHANTER: PHysical layer and Access Node TEchnology Revolutions: enabling the next generation broadband network. The scientific responsibility is assumed by its authors.

R. B. Moraes, P. Tsiaflakis and M. Moonen are with the Department of Electrical Engineering (ESAT-SCD/SISTA), KU Leuven, Kasteelpark Arenberg 10, B-3001 Leuven, Belgium. P. Tsiaflakis is funded by the Research Foundation-Flanders (FWO) (e-mail: rodrigo.moraes@esat.kuleuven.be; paschalis.tsiaflakis@esat.kuleuven.be; and marc.moonen@esat.kuleuven.be).

I. Introduction

Digital Subscriber Line (DSL) is today one of the main technologies for broadband access. Recently, there has been a strong activity in the research community to deal with DSL's main problems. One such area of research is focused on the optimal allocation of per-user power so that the impact of multi-user *crosstalk*, the main source of performance degradation for DSL, is minimized and the capabilities of the network are maximized. This is referred to as dynamic spectrum management (DSM). Work on DSM has progressed significantly in the past decade. Today, some near optimal, semi-centralized, trustworthy and low complexity solutions exist, e.g. [1]–[5].

Most of this previous work considers a synchronous discrete multitone (DMT) model, one in which all users have their DMT blocks perfectly synchronized. This leads to crosstalk decoupled across tones, i.e. crosstalk that can be dealt with on a per-tone basis. This assumption simplifies the DSM optimization problem significantly. However, the synchronous DMT model may not be very realistic in practice. There are some proposals to overcome the asynchronicity of the DMT blocks by adding a cyclic suffix [6], but it must be said that the conditions for synchronous DMT transmission may not always be easy to attain. Situations where interfering users belong to different service providers or where transmitters are not co-located are especially troublesome. In this correspondence we therefore focus on the *asynchronous* DSM problem [1], [2], [7].

The consequence of the time offset between the DMT blocks from different users is inter-carrier interference (ICI). With ICI, the crosstalk decoupling is broken: a tone of an interferer user affects not only the corresponding tone of a victim user, but all neighboring tones too. One fundamental step for solving the asynchronous DSM problem is an accurate characterization of the ICI. Such characterization entails calculating the ICI coefficients $\gamma_{n,i}^{k,j}\ \forall n,i,q,k,\ n \neq i$, which correspond to the crosstalk that power loaded on user i on tone j causes to user n on tone k. Most high quality DSM algorithms need these coefficients for the solution of the problem. Approximate characterizations lead to inaccurate power allocation, which in turn leads to suboptimal performance.

The main contribution of this correspondence is the derivation an accurate model for the ICI, one that takes into account all peculiarities of DMT transmission. We take into account ICI coefficients dependent on the specific delay between two users and ICI coefficients averaged over the delays between two users. We show that an accurate characterization of the ICI has a positive impact on the final performance of the system.

This paper is organized as following: Section II presents the problem of interest and a brief summary

of the previous work; Section III derives the novel model for the ICI; Section IV contains experimental results; and finally Section V presents final remarks.

II. Problem Statement and Previous Work

Consider an N user DMT system with K Δ_f-spaced tones and let $\mathbf{P} = \{p_n^k\} \in \mathbb{R}^{K\times N}$ be a matrix in which p_n^k is the transmit power of user n on tone k. Let $\tilde{\sigma}_n^k$ be the background noise power observed by the user n on tone k, $h_{n,i}^k$ be the channel gain between transmitter i and receiver n at tone k and Γ be the SNR gap to capacity. The bit loading for user n on tone k in the asynchronous case is defined as

$$b_n^k = \log\left(1 + \frac{p_n^k}{\sigma_n^k + \mathrm{XT}_n^k}\right)$$

where

$$\mathrm{XT}_n^k = \sum_{i\neq n}^{N}\sum_{j=1}^{K} \alpha_{n,i}^{k,j} p_i^j, \tag{1}$$

$$\alpha_{n,i}^{k,j} = \frac{\Gamma\gamma_{n,i}^{k,j}|h_{n,i}^j|^2}{|h_{n,n}^k|^2} \tag{2}$$

We use $\log$ to denote base two logarithm. Also $\sigma_n^k = \Gamma\tilde{\sigma}_n^k(|h_{n,n}^k|^2)^{-1}$. In (2), $\alpha_{n,i}^{k,j}$ and $\gamma_{n,i}^{k,j}$ are respectively, the normalized channel gain and the ICI coefficient specifically from user i to user n, and from tone j to tone k. The variable XT_n^k in (1) is the total crosstalk for user n on tone k. For the synchronous case, $\gamma_{n,i}^{k,j} = 1$ for $k = j$ and zero otherwise for all users and tones. The data rate for user n is given by $R_n = f_s\sum_k b_n^k$, where f_s is the symbol rate.

The DSM problem of interest is that of finding a matrix $\hat{\mathbf{P}}$ that maximizes data rates of all users in the network given a power budget for each user. This problem is called rate adaptive (RA). In mathematical form, it can be written as the maximization of the weighted rates i.e.

$$\hat{\mathbf{P}} = \arg\max_{\mathbf{P}} \sum_n w_n R_n$$

$$\text{subject to} \quad \sum_k p_n^k \leq P_n^{\max}\ \forall n$$

The weight w_n can be interpreted as a priority given to user n.

Previous work on the asynchronous DSM problem includes three alternative solutions [1], [2], [7]. We will describe what seems to be the most efficient of these solutions, the modified iterative waterfilling (MIW) [1], in more detail in Section IV, particularly in how this algorithm depends on the ICI coefficients.

Our goal is the accurate characterization of the ICI coefficients and an assessment of how it impacts the DSM problem. For single-user systems, the modeling of the ICI and inter-symbol interference due

to an insufficient cyclic prefix length is well studied in the literature (e.g. [8]). Here, we focus on an ICI that emerges for another reason, namely the asynchronism between different users sharing the DSL network. This phenomenon was first studied by Chan and Yu [7] and all subsequent works followed their model. Referring to Fig. 1, consider two non-synchronized users. The delay is η, $0 \leq \eta \leq 1$, indicating a fraction of the DMT block length. According to [7], the ICI coefficients as a function of η are given by

$$\gamma_{n,i}^{k,j} = \begin{cases} \frac{(\eta K)^2 + (K - \eta K)^2}{K^2}, & j = k; \\ \dfrac{2\sin^2(\pi(k-j)\eta)}{K^2 \sin^2(\pi/K(k-j))}, & j = 1, \ldots, K,\ j \neq k. \end{cases} \tag{3}$$

The authors of [7] also consider a worst case, in which the coefficients do not depend on the delay and are given by

$$\gamma_{n,i}^{k,j} = \begin{cases} 1, & j = k; \\ \dfrac{2}{K^2 \sin^2(\pi/K(k-j))}, & j = 1, \ldots, K,\ j \neq k. \end{cases} \tag{4}$$

The derivation of (3) and (4) involves a few approximations. For example, the ICI coefficients are not user dependent—thus we could drop the subscripts i and n, but we keep the same notation as in (2) for consistency—and the cyclic prefix between consecutive blocks is not considered. Also note that the ICI coefficients are symmetric, i.e $\gamma_{n,i}^{(j-k),j} = \gamma_{n,i}^{j+k,j}$. To the best of our knowledge, this is so far the only attempt to calculate the ICI coefficients.

III. Derivation of ICI Coefficients

This section is divided in two parts. First, we obtain the ICI coefficients as a function of the delay η. Second, we obtain the ICI coefficients averaged over η.

In the following, lower-case boldface letters denote vectors, while upper-case boldface is used for matrices. When we refer to DMT symbols, bracketed subscripts refer to time (not to user) and superscripts to tones. Hence $a_{(i)}^{k}$ should be read as a quantity in the ith block at the kth tone. The vector $\mathbf{a}_{(i)} = \begin{bmatrix} a_{(i)}^{1} & \cdots & a_{(i)}^{K} \end{bmatrix}^{\mathrm{T}}$ is representative for the ith symbol. The DMT block has length $K + L_{\mathrm{cp}}$, where L_{cp} is the length of the cyclic prefix (CP)—we refer to a block as the symbol plus the CP. Other notation includes $\mathrm{E}[\cdot]$ as expectation, $(\cdot)^{\mathrm{H}}$ as conjugate transpose, $\lfloor \cdot \rfloor$ as rounding down and $\mathrm{diag}\{\mathbf{a}\}$ as a matrix with $\mathbf{a}$ on the main diagonal. Also $\mathbf{0}_{N \times K}$ is the $N \times K$ matrix of zeros and $\mathbf{I}_K$ is the $K \times K$ identity matrix.

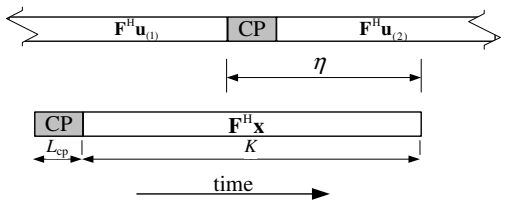

Fig. 1. DMT reception in time for victim user n.

A. ICI coefficients as a function of the delay η

Referring to Fig. 1, we consider a victim user n and one interferer i. The victim user has DMT symbol denoted by $\mathbf{x} \in \mathbb{C}^K$, while the interferer is represented by $\mathbf{u} \in \mathbb{C}^K$. Users are not synchronized, and the delay is η, $0 \leq \eta \leq 1$, indicating a fraction of the DMT block length. We define η as the delay between the beginning of the CP of the interferer to the end of the DMT block of the vicim user user (see Fig. 1). DMT symbols $\mathbf{u}_{(1)}$ and $\mathbf{u}_{(2)}$ interfere with the reception of the victim user. Mathematically, reception for the victim user is given by

$$\begin{aligned} \mathbf{r} &= \mathbf{F}\widetilde{\mathbf{C}}\mathbf{G}_{n,n}\mathbf{C}\mathbf{F}^{\mathrm{H}}\mathbf{x} + \mathbf{F}\widetilde{\mathbf{C}}\mathbf{G}_{n,i}\mathbf{S}_{(1)}\mathbf{C}\mathbf{F}^{\mathrm{H}}\mathbf{u}_{(1)} + \mathbf{F}\widetilde{\mathbf{C}}\mathbf{G}_{n,i}\mathbf{S}_{(2)}\mathbf{C}\mathbf{F}^{\mathrm{H}}\mathbf{u}_{(2)} + \mathbf{z} \\ &= \mathrm{diag}\left\{\mathbf{h}_{n,n}\right\}\mathbf{x} + \mathbf{F}\widetilde{\mathbf{C}}\mathbf{G}_{n,i}\mathbf{S}_{(1)}\mathbf{C}\mathbf{F}^{\mathrm{H}}\mathbf{u}_{(1)} + \mathbf{F}\widetilde{\mathbf{C}}\mathbf{G}_{n,i}\mathbf{S}_{(2)}\mathbf{C}\mathbf{F}^{\mathrm{H}}\mathbf{u}_{(2)} + \mathbf{z}. \end{aligned} \tag{5}$$

Here $\mathbf{F}$ and $\mathbf{F}^{\mathrm{H}} \in \mathbb{C}^{K\times K}$ represent the DFT and IDFT matrices, respectively; $\mathbf{G}_{n,i} \in \mathbb{C}^{(K+L_{\mathrm{cp}})\times(K+L_{\mathrm{cp}})}$ is a Toeplitz matrix with first column $\left[\mathbf{g}_{n,i}^{\mathrm{T}}\ \mathbf{0}_{1\times(K+L_{\mathrm{cp}}-L)}\right]^{\mathrm{T}}$and first row $\left[g_{n,i}(1)\ \mathbf{0}_{1\times(K+L_{\mathrm{cp}}-1)}\right]$, where $\mathbf{g}_{n,i} \in \mathbb{C}^L$ is the L-tap channel impulse response from transmitter i to receiver n and is considered constant in time; $\mathbf{h}_{n,i} = \left[h_{n,i}^1\ \cdots\ h_{n,i}^K\right]^{\mathrm{T}} \in \mathbb{C}^K$ is the corresponding channel frequency response; $\mathbf{z} \in \mathbb{C}^K$ is the background Gaussian noise vector; and the matrices

$$\widetilde{\mathbf{C}} = \left[\begin{array}{c:c} \mathbf{0}_{K\times L_{\mathrm{cp}}} & \mathbf{I}_K \end{array}\right]$$

and

$$\mathbf{C} = \left[\begin{array}{c:c} \mathbf{0}_{L_{\mathrm{cp}}\times(K-L_{\mathrm{cp}})} & \mathbf{I}_{L_{\mathrm{cp}}} \\ \hdashline \multicolumn{2}{c}{\mathbf{I}_K} \end{array}\right],$$

where $\widetilde{\mathbf{C}} \in \mathbb{N}^{K\times(K+L_{\mathrm{cp}})}$ and $\mathbf{C} \in \mathbb{N}^{(K+L_{\mathrm{cp}})\times K}$, respectively remove and insert the CP. If $L_{\mathrm{cp}} \geq L$, the operation $\widetilde{\mathbf{C}}\mathbf{G}_{n,n}\mathbf{C}$ results in a square circulant matrix, which is then diagonalized by pre- and post-multiplication with the IDFT and DFT matrices. We assume that the CP is longer than both the direct and crosstalk channel impulse responses.

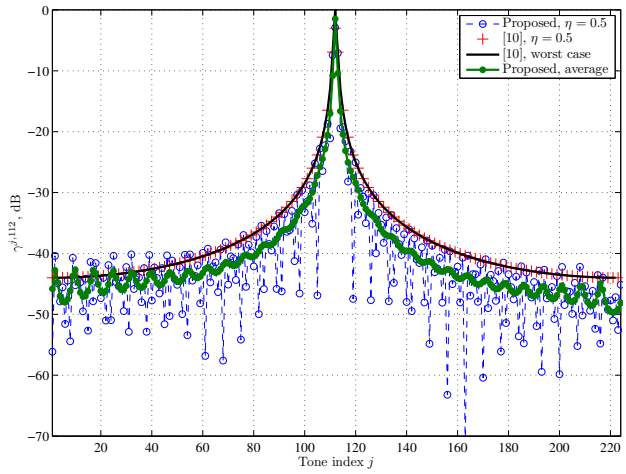

Fig. 2. ICI coefficients from (12), (3) and from (4). For the fisrt two plots, $\eta = 0.5$. The crosstalk channel is 1 km long.

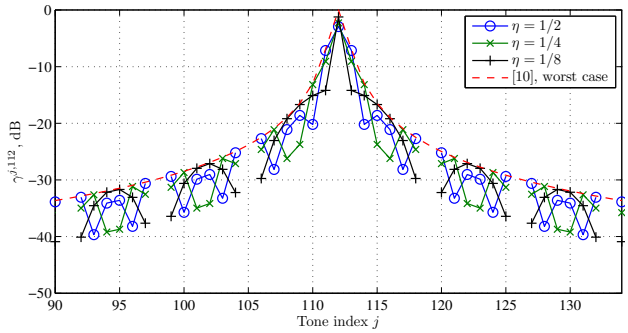

Fig. 3. ICI coefficients for different values of the delay η. In this plot we consider a frequency flat channel.

The matrices $\mathbf{S}_{(1)}$ and $\mathbf{S}_{(2)}$ capture the effect of the time offset. Define $\omega = \lfloor \eta(K + L_{\rm cp}) \rfloor$ as the number of samples in delay, then these matrices are given by

$$\mathbf{S}_{(1)} = \left[\begin{array}{c|c} \mathbf{0}_{(K+L_{\rm cp}-\omega)\times\omega} & \mathbf{I}_{(K+L_{\rm cp}-\omega)} \\ \hline \multicolumn{2}{c}{\mathbf{0}_{\omega\times(K+L_{\rm cp})}} \end{array}\right] \tag{6}$$

and

$$\mathbf{S}_{(2)} = \left[\begin{array}{c} \mathbf{0}_{(K+L_{\rm cp}-\omega)\times(K+L_{\rm cp})} \\ \hline \mathbf{I}_{\omega} \quad \mathbf{0}_{\omega\times(K+L_{\rm cp}-\omega)} \end{array}\right]. \tag{7}$$

Here $\mathbf{S}_{(1)},\ \mathbf{S}_{(2)} \in \mathbb{N}^{(K+L_{\rm cp})\times(K+L_{\rm cp})}$. If η is equal to zero or one, then the system is synchronized and $\mathbf{S}_{(1)} = \mathbf{I}_{(K+L_{\rm cp})}$ and $\mathbf{S}_{(2)} = \mathbf{0}_{(K+L_{\rm cp})\times(K+L_{\rm cp})}$ or vice-versa. For $0 < \eta < 1$, the operation $\widetilde{\mathbf{C}}\mathbf{G}_{n,i}\mathbf{S}_{(1)}\mathbf{C}$ (and $\widetilde{\mathbf{C}}\mathbf{G}_{n,i}\mathbf{S}_{(2)}\mathbf{C}$) fails to produce a circulant matrix, and therein lies the effect of the asynchronicity.

Observe that we can write one element of $\mathbf{r}$ in (5) as

$$r^k = h^k_{n,n}x^k + \sum_j \mathbf{A}[k,j]u^j_{(1)} + \sum_j \mathbf{B}[k,j]u^j_{(2)} + z^k, \tag{8}$$

where we define

$$\mathbf{A} = \mathbf{F}\widetilde{\mathbf{C}}\mathbf{G}_{n,i}\mathbf{S}_{(1)}\mathbf{C}\mathbf{F}^{\mathrm{H}}, \tag{9}$$

$$\mathbf{B} = \mathbf{F}\widetilde{\mathbf{C}}\mathbf{G}_{n,i}\mathbf{S}_{(2)}\mathbf{C}\mathbf{F}^{\mathrm{H}}. \tag{10}$$

In (8), the $[k,j]$ elements of $\mathbf{A}$ and $\mathbf{B}$ account for the ICI effect when $j \neq k$.

With (9) and (10) in hands and taking into account that the PSD of the crosstalk symbols is $\mathrm{E}\left[\mathbf{u}_{(1)}\mathbf{u}^{\mathrm{H}}_{(1)}\right] = \mathrm{E}\left[\mathbf{u}_{(2)}\mathbf{u}^{\mathrm{H}}_{(2)}\right] = \mathrm{diag}\left\{\mathbf{p}_i\right\}$, we can write

$$\gamma^{k,j}_{n,i}|h^j_{n,i}|^2 p^j_i = \left(|\mathbf{A}[k,j]|^2 + |\mathbf{B}[k,j]|^2\right) p^j_i. \tag{11}$$

Eq. (11) is easily calculable and it offers an accurate model for the ICI as a function of $\mathbf{g}_{n,i}$ and η.

However, for comparing the ICI coefficients to those of [7], we want the ICI PSD to be captured by a multiplication of the type $\mathbf{M}_{n,i}\mathrm{diag}\left\{|\mathbf{h}_{n,i}|^2\right\}\mathrm{diag}\left\{\mathbf{p}_i\right\}$, where $\mathbf{M}_{n,i} \in \mathbb{R}^{K\times K}$ is the ICI coefficients matrix and $|\mathbf{h}_{n,i}|^2 = \left[|h^1_{n,i}|^2 \ \cdots \ |h^K_{n,i}|^2\right]^{\mathrm{T}} \in \mathbb{R}^K$. If we follow the notation of [7], each row of $\mathbf{M}_{n,i}$ would contain the ICI coefficients for one victim tone, i.e. $\mathbf{M}_{n,i} = \left[\boldsymbol{\gamma}^1_{n,i}\ \boldsymbol{\gamma}^2_{n,i}\ \cdots\ \boldsymbol{\gamma}^K_{n,i}\right]$, where $\boldsymbol{\gamma}^k_{n,i} = \left[\gamma^{1,k}_{n,i}\ \cdots\ \gamma^{K,k}_{n,i}\right]^{\mathrm{T}}$. Calculating the PSD of the interference term in (5), we obtain

$$\mathbf{M}_{n,i}\mathrm{diag}\left\{|\mathbf{h}_{n,i}|^2\right\}\mathrm{diag}\left\{\mathbf{p}_i\right\} = \left(|\mathbf{F}\widetilde{\mathbf{C}}\mathbf{G}_{n,i}\mathbf{S}_{(1)}\mathbf{C}\mathbf{F}^{\mathrm{H}}|^2 + |\mathbf{F}\widetilde{\mathbf{C}}\mathbf{G}_{n,i}\mathbf{S}_{(2)}\mathbf{C}\mathbf{F}^{\mathrm{H}}|^2\right)\mathrm{diag}\left\{\mathbf{p}_i\right\},$$

and hence

$$\mathbf{M}_{n,i} = \left(|\mathbf{A}|^2 + |\mathbf{B}|^2\right)\mathrm{diag}\left\{|\mathbf{h}_{n,i}|^2\right\}^{-1}, \tag{12}$$

where $\mathbf{A}$ and $\mathbf{B}$ are defined in (9) and (10) and where the $[k,j]$th element of $|\mathbf{A}|$ is $|\mathbf{A}[k,j]|$.

With $\mathbf{M}_{n,i}$ calculated as in (12) we can calculate $\alpha^{k,j}_{n,i}$ with (2) and crosstalk (1). Notice in both (11) and (12) that we need the crosstalk channel impulse response, $\mathbf{g}_{n,i}$, to compute (11) or (12).[1] As a consequence, the *ICI coefficients are channel dependent*, i.e. different crosstalk channels have different ICI coefficients. They are also frequency dependent: The lines of $\mathbf{M}_{n,i}$ are similar, but they are not delayed replicas of one another, e.g. $\gamma^{k,j}_{n,i}$ is usually slightly different than $\gamma^{k+1,j+1}_{n,i}$. It can be shown that the only exception to these two facts is the case of frequency flat channels, i.e. when $\mathbf{g}_{n,i} = \left[\nu\ \mathbf{0}_{K+L_{\mathrm{cp}}-1\times 1}\right]^{\mathrm{T}}$

[1]Notice that if the channel frequency response is for some tone close to being zero, i.e. for some k, $h^k_{n,i} \approx 0$, calculating (12) might be inaccurate. However, even in this case (11) offers an accurate model for the ICI.

for a given complex number ν. Notice that in this case $\mathbf{G}_{n,i} = \nu \mathbf{I}_K$. For the frequency flat case, they are also not frequency dependent, i.e. $\gamma_{n,i}^{k,j} = \gamma_{n,i}^{k+1,j+1}$.

In Fig. 2, we plot the ICI coefficients for tone 112 of the 224 tones of an ADSL downstream system with AWG 24 cable for a delay of $\eta = 0.5$. The crosstalk channel for this example is 1 km long and was calculated according to [9]. We use a CP of 32 samples [10]. The plot shows ICI coefficients calculated with (3) and (4), following the model of [7]; and (12) in this correspondence. Observe that the coefficients of (3) for $\eta = 0.5$ are usually optimistic and the coefficients of (4) for the worst case are usually pessimistic. For instance, for the coefficients of (3) for $\eta = 0.5$ every second tone has coefficient equal to zero. For the worst case, in certain tones the difference between the coefficients in (4) and (12) is more than 25 dB. Also note that, although there are many similarities, the ICI coefficients calculated with (12) are not perfectly symmetric.

In Fig. 3, we illustrate the change in the coefficients when we vary η for tone 112 of the 224 tones for the same ADSL system. For this plot, we assume a frequency flat crosstalk channel. We also only show the ICI coefficients of the 12 closest tones. As mentioned, the coefficients are now symmetric and not frequency dependent. In the figure, we can better see how the ICI coefficients spread power in frequency as η increases. The case with $\eta = 0.5$ is where the coefficients are the most spread. For this case, the direct coefficients are approximately -3 dB and the neighboring coefficients are about -7.1 dB. For $\eta = 1/4$, these values are, respectively, -2.3 and -9.1 dB. For $\eta = 1/8$, we obtain -1.2 and -14.1 dB. In this same figure, we again show the worst case model of (4).

B. ICI coefficients averaged over η

On the previous section η was considered a fixed variable. In this section, we consider it to be a random variable, and we calculate the crosstalk as the expected value of a function of η. Let $\mathbf{M}_{n,i}(\eta)$ be a function of the random variable η. It is defined similarly to (12), i.e.

$$\mathbf{M}_{n,i}(\eta) = \left(|\mathbf{A}|^2 + |\mathbf{B}^2|\right) \operatorname{diag}\{|\mathbf{h}_{n,i}|^2\}^{-1}.$$

We remind that the dependence on the delay η is through the definition of (6) and (7). Also, let $f_\eta(H)$ be a given probability distribution function. The expected value of a function of a random variable is given by the inner product of the function and the probability density function of the random variable (see [11], Eq. 5-55), i.e.

$$\mathrm{E}\left[\mathbf{M}_{n,i}(\eta)\right] = \int_{-\infty}^{+\infty} \mathbf{M}_{n,i}(H) f_\eta(H) dH. \tag{13}$$

We can rewrite (13) in a more convenient form by noticing that the matrices $\mathbf{S}_{(1)}$ and $\mathbf{S}_{(2)}$ in (6) and (7) depend on $\lfloor \eta(K+L_{\rm cp}) \rfloor$. Hence, we define a discrete random variable $\omega = \lfloor \eta(K+L_{\rm cp}) \rfloor$. We consider that η is uniformly distributed between 0 and 1, which leads us to conclude that ω is also uniformly distributed. Mathematically, we have $\Pr(\omega = \Omega) = {}^1\!/_{K+L_{\rm cp}},\ \Omega = \{0, 1, \ldots, K+L_{\rm cp}-1\}$. In this way, we can rewrite (13) as a simple average, i.e.

$$\widetilde{\mathbf{M}}_{n,i} \triangleq \mathrm{E}\left[\mathbf{M}_{n,i}(\omega)\right] = \sum_{\Omega=0}^{K+L_{\rm cp}-1} \mathbf{M}_{n,i}(\Omega) \frac{1}{K+L_{\rm cp}}. \tag{14}$$

With $\widetilde{\mathbf{M}}_{n,i}$ in hands, we can calculate crosstalk with (2) and (1). In Fig. 2, we plot the ICI coefficients of (14) for tone 112 of the same 1 km crosstalk channel mentioned on Section III-A.

Eq. (14) is useful because it is independent of the specific delay between two users. In practice calculating the ICI coefficients with (14) may be more interesting, since it is likely that the delay between the transmission of two users changes over time and is not known accurately. Here, we take an approach of assuming we know nothing about the delay, and thus we assume the probability distribution of η to be uniform. Other options are possible.

Because the delay is a source of uncertainty, using the ICI coefficients in (14) adds some robustness to the subsequent PSD design—we will see an example of that in Section IV. Recently, other such sources of uncertainty in the parameters of the problem were considered. For example, [12] deals with the impact of errors in the direct and crosstalk channel estimation. Here, we consider all channel transfer functions, both direct and crosstalk, to be known perfectly.

IV. Experiments

In this section, we illustrate how an accurate characterization of the ICI coefficients impacts on performance. For assessing this impact, we need a DSM algorithm for solving the asynchronous problem. Our choice is the MIW [1]. We choose this algorithm for a couple of reasons. The MIW has been shown to outperform the algorithms in [2], [7] and has reasonable computational complexity. This solution is based on solving the Karush-Kuhn-Tucker (KKT) stationarity conditions so that powers are found for every user and tone; and then updating an interference-dependent term that should be taken into account for the next iteration of power allocation.

Power allocation for the MIW is done with the formula

$$p_i^j = \frac{w_i}{\lambda_i + t_i^j} - (\sigma_i^j + \mathrm{XT}_i^j), \tag{15}$$

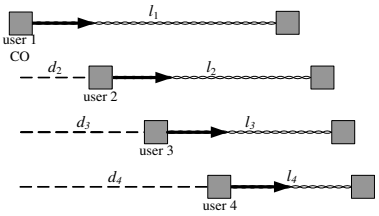

Fig. 4. Near-far downstream ADSL scenario.

where

$$t_i^j = \sum_{n \neq i} w_n \sum_k \frac{\alpha_{n,i}^{k,j} (\mathrm{SINR}_n^k)^2}{p_n^k (\mathrm{SINR}_n^k + 1)} \tag{16}$$

Here $\mathrm{SINR}_n^k = p_n^k \left(\sigma_n^k + \mathrm{XT}_n^k\right)^{-1}$. In (15), λ_n is a Lagrange multiplier that should be adjusted so that the power budget is respected. The variable t_i^q is a per-tone penalty that distorts the waterfilling formula so that damage to other users is considered. Eq. (15) should be applied iteratively and should jointly hold for all users and tones in the network.

The MIW can be applied in a distributed fashion in the network. Users can apply (15) locally. After power allocation, they should measure their SINR's, calculate $(\mathrm{SINR}_n^k)^2 \left(p_n^k (\mathrm{SINR}_n^k + 1)\right)^{-1}$ for every tone and send these values to a spectrum management center (SMC). The SMC then calculates the per-tone penalties with (16) for all users and tones and sends these values to the users. Note that users can measure their SNIR's accurately without the knowledge of the ICI coefficients, but the SMC needs accurate values for the ICI coefficients $\gamma_{n,i}^{k,j}$, which in turn define $\alpha_{n,i}^{k,j}$ (see (16) and (2)). Inaccurate ICI coefficients on the SMC can lead to inaccurate values for the per-tone penalties, which in turn influences the power allocation and performance.

In this section, we will assess the performance of the MIW for three cases. First, we consider the case when the delay η is known for every user pair, the accurate ICI coefficients are calculated with (12) and used at the SMC; second, we consider the case when the delay is not known, the averaged ICI coefficients are calculated with (14) and used at the SMC; and, third, we consider the case when the delay is not known, the worst case ICI coefficients in (4) are calculated and used at the SMC.

All simulations in this section consider downstream ADSL. Cables of 0.5 mm (AWG 24) are used and an SNR gap of 12.8 dB is considered. Modems have at their disposal a maximum power of 20.4 dBm. For each line, noise model ANSI A is adopted.

We consider the near-far downstream ADSL scenario with 4 users depicted in Fig. 4. Define the vectors $\mathbf{l} = \begin{bmatrix} l_1 & \cdots & l_4 \end{bmatrix}^{\mathrm{T}}$, $\mathbf{d} = \begin{bmatrix} d_1 & \cdots & d_4 \end{bmatrix}^{\mathrm{T}}$, shown in Fig. 4. We thus set the scenario as $\mathbf{l} = \begin{bmatrix} 5 & 4 & 3.5 & 3 \end{bmatrix}^{\mathrm{T}}$ km

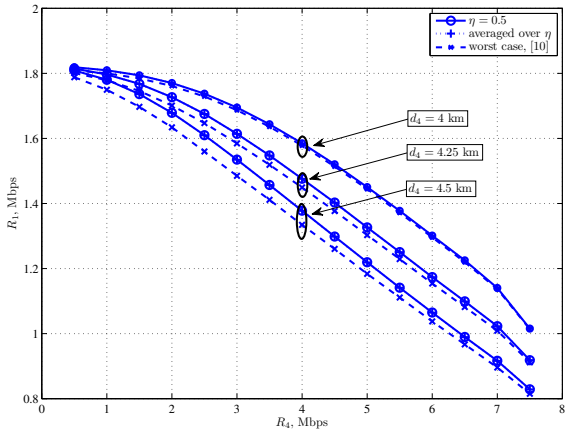

Fig. 5. Rate region for a scenario with $\mathbf{l} = [5 \;\; 4 \;\; 3.5 \;\; 3]^{\mathrm{T}}$ km and $\mathbf{d} = [0 \;\; 2 \;\; 3 \;\; d_4]^{\mathrm{T}}$ km, where d_4 takes the values of 4, 4.25 and 4.5 km. For all point in the RR we set $R_2 = 2$ Mbps and $R_3 = 3$ Mbps.

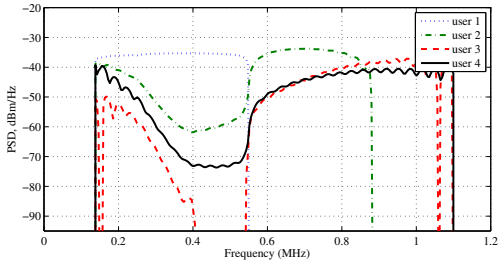

Fig. 6. PSDs corresponding to the point $R_4 = 5$ Mbps with $d_4 = 4.5$ km for the RR in Fig. 5

and $\mathbf{d} = \begin{bmatrix} 0 & 2 & 3 & d_4 \end{bmatrix}^{\mathrm{T}}$ km. We simulate three different values for d_4, $d_4 = 4$, $d_4 = 4.25$ and $d_4 = 4.5$ km.

Consider the delay between user i and n to be given by $\eta_{n,i}$. We consider users 1 and 2 to be synchronized, so $\eta_{1,2} = \eta_{2,1} = 0$. We also consider $\eta_{3,4} = \eta_{4,3} = 0$. Users 1 and 2 have a delay of 0.5 in relation to users 3 and 4, so $\eta_{4,1} = \eta_{1,4} = 0.5$, $\eta_{3,2} = \eta_{2,3} = 0.5$ and so on.

We depict the rate regions for the three cases of interest regarding the knowledge of the ICI coefficients on the SMC and for the three different values of d_4 in Fig. 5 . For all points, we have $R_2 = 2$ Mbps and $R_3 = 3$ Mbps. As we can see from the plot, using the averaged ICI coefficients on the SMC provides performance which is practically the same as that using the actual coefficients. This suggests that the accurate values may not be all the time strictly necessary. Performance is clearly worse with the worst case ICI coefficients. These coefficients are too pessimistic, and lead to per-tone penalties which are somewhat exaggerated.

For $R_4 = 5$ Mbps, we plot the resulting power allocation for the case when the SMC has the actual

coefficients in Fig. 6. A particularly interesting observation for the asynchronous case is the gently increasing transmit powers for users 3 and 4 after user 1 stops transmission. For a synchronous scenario, the transmit power changes abruptly, i.e. as soon as user 1 stops transmission, other users can transmit at full power. The ripples on the power allocation in Fig. 6 are due to the ICI coefficients.

V. Conclusion

Previous work on DSM has mostly focused on the synchronous transmission case, which makes the problem easier but may not be very realistic in practice. In this correspondence, we have focused on the asynchronous DSM problem. We have provided an accurate ICI characterization for the asynchronous DMT transmission in DSL networks. We also have provided an ICI characterization averaged over the possible delays between two users. An accurate ICI characterization provides more solid foundations for further research on this topic. Also, simulation results show that an accurate characterization of the ICI coefficients can have a positive impact on the performance of distributed DSM algorithms.

References

[1] W. Yu, "Multiuser water-filling in the presence of crosstalk," in *Inf. Theory and Appl. Workshop*, San Diego, USA, 2007.

[2] R. Cendrillon, J. Huang, M. Chiang, and M. Moonen, "Autonomous spectrum balancing for digital subscriber lines," *IEEE Trans. Signal Process.*, vol. 55, no. 8, pp. 4241–4257, 2007.

[3] P. Tsiaflakis, M. Diehl, and M. Moonen, "Distributed spectrum management algorithms for multiuser DSL networks," *IEEE Trans. Signal Process.*, vol. 56, no. 10, pp. 4825–4843, 2008.

[4] R. B. Moraes, B. Dortschy, A. Klautau, and J. R. i Riu, "Semiblind spectrum balancing for DSL," *IEEE Trans. Signal Process.*, vol. 58, no. 7, pp. 3717–3727, 2010.

[5] J. Papandriopoulos and J. S. Evans, "SCALE: a low-complexity distributed protocol for spectrum balancing in multiuser DSL networks," *IEEE Trans. Inf. Theory*, vol. 55, no. 8, pp. 3711–3724, 2009.

[6] F. Sjöberg, M. Isaksson, R. Nilsson, P. Ödling, S. K. Wilson, , and P. O. Börjesson, "Zipper: A duplex method for VDSL based on DMT," *IEEE Trans. Commun.*, vol. 47, no. 8, pp. 1245–1252, 1999.

[7] V. M. K. Chan and W. Yu, "Multiuser spectrum optimization for discrete multitone systems with asynchronous crosstalk," *IEEE Trans. Signal Process.*, vol. 55, no. 11, pp. 5425–5435, 2007.

[8] W. Henkel, G. Tauböck, P. Ödling, P. O. Börjesson, and N. Petersson, "The cyclic prefix of OFDM/DMT—an analysis," in *Int. Zurich Seminar on Broadband Commun.*, Zurich, Switzerland, 2002.

[9] ETSI Std. TS 101 270-1, "Transmission and multiplexing (TM); acess transmission systems on matellic acess cables; very-high bit-rate digital subscriber line transceivers (VDSL); part 1: Functional requirements," 2003.

[10] ITU std. G.992.2, "Asymmetrical digital subscriber line transceivers 2 (ADSL2)," 2002.

[11] A. Papoulis and S. U. Pillai, *Probability, Random Variables and Stochastic Processes*, 4th ed. McGraw-Hill Inc., New York, 2001.

[12] N. Lindqvist, F. Lindqvist, B. Dortschy, E. Pelaes, and A. Klautau, "Impact of crosstalk estimation on the dynamic spectrum management performance," in *IEEE Global Telecommun. Conf.*, New Orleans, USA, 2008.